Appendices

Annex 1 List of Abbreviations and Symbols

Polymers

PVA	Polyvinyl alcohol
PAA	Poly(acrylic acid)
P(VDF-TrFE)	Poly(vinylidenefluoride-co-trifluoroethylene)
PEG	Poly (ethylene glycol)
PVDF	Poly(vinylidene fluoride)
PMMA	Poly (methylmethacrylate)
PDA	Polydopamine
PES	Polyethersulfone
PSf	Polysulfone
DA	Dopamine
PEGMA	Poly(ethylene glycol) methyl ether methacrylate
CA	Cellulose Acetate

Pollutant

MB	Methylene Blue
IBPR	Ibuprofen
DS	Dichlofenac Sodium
MO	Methyl Orange
RB	Reactive Blue
RdB	Rodamine B
RB5	Reactive black 5
BSA	Bovine Serum Albumin
BG	Brilliant green
BPA	Bisphenol A
EE2	17α-ethynylestradiol
HA	Humic Acid
POME	Palm oil mill effluent
NP	Nonylphenol
Tartz	Tartzarine
SULF	Sulfadiazine
Ind. Surf	Industrial Surfactant
EY	Eosin Yellow
SFMO	Sulfamethoxazole
Bentz	Bentazon

Solvent and other additives

NMP	1-Methyl-2-pyrrolidone
DMF	N,N-dimethylformamide
mpg-C_3N_4	Mesoporous graphitic carbon nitride
DMAc	N,N- dimethyl acetamide
TTIP	Titanium tetraisopropoxide
EtOH	Ethanol
APTES	Aminopropyltriethoxysilane
TEP	triethyl phosphate
RGO	Reduced Graphene Oxide
GLUT	Glutaraldehyde

Others

HF	Hollow Fiber
DHLF	Dual Layer Hollow Fiber Membrane
N.D.	Not Detectable
ALD	Atomic Layer Deposition

List of Symbols

θ	Contact Angle
ε	Porosity
Model	Model pollutant
V_0	Volume of contaminated solution
C_0	Initial concentration
D	Degradation
R	Rejection
k_{app}	Apparent reaction kinetic constant
A	Area of the membrane
I	Irradiation source and power
t	Total irradiation time
P	Performance in terms of µg of pollutant removed per hour per area of PMs
υ	Recirculation velocity

Annex 2 UV-responsive PMs used in different types of PMRs, their Photocatalytic Activity and other membrane performances with operating conditions

Annex 3 Batch PMRs Using Flat Sheet PMs

PM type	wt% TiO_2 added	θ (°)		ε (%)		M	C_0 , V_0, pH,	I, t, A	D (%)	k_{app} (min^{-1})	P (μg/(h× cm^2))	Observation and other performances	Ref.
		PVDF	PM	PVDF	PM								
TiO_2/PVDF(2 mM TTIP/ EtOH sol-gel)	0.092 wt% of dry PMs	73	76	7% of porosity reduced		MB	3.2 mg/L, 4 mL	76 W/m^2 UV-A, 2.5 h, 4.12 cm^2.	100% (2 h)		1.55	Decrease hydrophlicity and porosityof PMs and hence water flux decreased but BSA filtration performance improved	[16]
						IBRF	100 mg/L, 4 mL		45 %		48.5		
						DS	25 mg/L, 4 mL		70%		12.13		
PVA/TiO_2/PVDF	1%	87	59	44	38	RB	50 mg/L, 150 ml	15W UV-C lamp, 2.5 h, 25 cm^2	44%	-	26.4	At optimum PVA (3 wt%) and 1 wt% TiO_2 improved mechanical property and hydrophilicty but above this value TiO_2 encapsulate.	[72]
						RdB			45%	-	27		
						MO			48%	-	28.8		
TiO_2/PAA/PVDF	0.5 (w/v)	116	28			RB5	40 mg/L, 25mL	15W UV lamp, 2 h, 25 cm^2	30%	0.031	6	Higher flux obtained under UV due to high antifouling property of the membrane. 3 wt% loading of TiO_2 shows best photocatalytic activity.	[28]
	1. 5 (w/v)		23						30%	0.033	6		
	3 (w/v)		N.D						42%	0.042	8		
TiO_2/PVP/PVDF/DMAc	1%	79	65	70	75	BSA	1000 mg/L, 50 mL.	11W UV, 2 h, 19.3 cm^2	53%	0.0068	686.5	Addition of TiO_2 decrease surface roughness, and incorporation GO faster the photodegradation of BSA and improve the BSA rejection and water flux.	[73]
GO/TiO_2/PVP/PVDF/DMAc	1%		61	70	83				80%	0.0142	1036.3		
TiO_2 nanotube/ PVP/PVDF/ DMAc	0.1%	92	82	28	43	BG	150 mL. pH 7.5,	15W Hg-lamp, 1.5 h, 50 cm^2.	42% for 1.5 wt%			Best antifouling property obtained for 1.5 wt% TiO_2 content, more than this porosity, mechanical stability and water flux decreased.	[74]
	0.5%		-		47								
	1.0%		73		50								
	1.5%		70		56								
	2%		-		36								
TiO_2/P(VDF–TrFE)/ DMF	3%	76	88	80	78	MB	3.2 mg/L, 13 mL, pH 6.8	40 W/m^2 LED UVA, 1.5 h, 12 cm^2	77%	0.018	1.78	8 wt% TiO_2 shows better photodegradation but porosity and hydrophilicity decreased. Inclusion of a zeolite (NaY) can increase hydrophilicity and porosity by aiding microporosity and capillary effect of zeolite.	[21]
	5%		97		77				93%	0.026	2.15		
	8%		97		74				99%	0.037	2.29		
NaY/TiO_2/P(VDF-TrFE) /DMF	3% NaY		N.D		90				91%	0.023	2.1		
	5% NaY				95				99%	0.04	2.29		
	8% NaY				97				96%	0.033	2.22		
TiO_2/PVDF/PMMA/PEG/PVP/TEP	0.12 %	110	102	82	80	MB	3.2 mg/L, 500 mL	500W UV lamp, 6.5 h, 16 cm^2	86%	0.0055	10.58	TiO_2 loading increase the porosity, hydrophilicity, and mechanical properties of PMs.	[75]
	0.25%		98		81				95%	0.0084	11.69		
	0.50%		93		83				99%	0.0117	12.18		
TiO_2/PVDF/PVP/DMAc	4%	108	61			MB	6.4 mg/L, 50 mL	UVA lamp 4W, 1.5 h, 20 cm^2	100 %	0.044	10.66	Fabrication of highly porous and photoactive PMs using a bipolymer system through electrospinning process.	[36]
						BPA	5.0 mg/L, 50 mL		96% (4 h)	0.030	3		
						EE2	5.0 mg/L, 50 mL		96%	0.033	8		

Annex 4 Continuous PMRs Using Flat Sheet PMs

Flat sheet (Dead End)

PM type	wt% TiO_2 added	θ (°)		ε (%)		M	C_0 , V_0, pH, υ	I, t, A	D (%) or R (%)	k_{app} (min^{-1})	Observation and other performances	Ref.
		PVDF	PM	PVDF	PM							
TiO_2/PVDF/H_2O	0.1 g/L**	128	127	75	34	RB 19	25 mg/L, pH 3, 0.877 L/min	9W UV-C, 1 h, 59.5 cm^2.	19%		Negatively charged RB5 favors acidic pH, alkaline condition decreases photoactivity.	[51]
	0.5 g/L		121		39				26%			
	1 g/L		114		40				35%			
TiO_2/PDA/PVDF	1.5 %	85	65	14	8	ARB	10 mL (cell)	0.12 W/m^2 UV lamp, 3 h, 4.1cm^2	98%		Increased hydrophilicity, and high antifouling properties	[20]
						ARGs			98%			
Flat sheet (Cross flow)												
TiO_2/PVDF (CVD)	-	61 90	26	70	-	MB	4.15 mg/L	6 W/m^2 Hg-lamp, 6 h, 14.5 cm^2	92% (4 h)	0.028	Needed to optimize sputtering conditions. Increased in hydrophilicity improved transmembrane fluxes.	[18]
						DS	29.6 mg/L, 250 mL/min		100%	0.0083		
TiO_2/PVP/PVDF/DA/DMAc	0.8%	80	30			SULF	100 µg/L, 100 mL. pH 7.5, 30 L/h	1.25 W/m^2 UV, 2 h, 26.12 cm^2.	91.4%	0.0216	Rejection increased under UV irradiation because of synergistic effect of photodegradation and filtration.	[44]
TiO_2/LiCl/PVDF/DMAc	0.5%		75			HA	2 mg/L, pH 7.5, 500 mL/min	100 W Hg-lamp, 8 h, 48 cm^2	82% of R		Better NOM rejection and reduction of membrane fouling with good self-cleaning ability.	[43]
Fe_3O_4@TiO_2/PVDF/NMP	0.5%	A decrease of 10° for PMs		1.5	1.6	HA	20 mg/L, 100 mL. pH 7.5, 100 L/h	19W Hg-lamp, 2 h, 50 cm^2.	67% of R		Most of the nanoparticles flocculate on the surface of PMs because of magnetic coagulation bath. Under UV, PMs had better antifouling performance against humic acid solution.	[76]
	1%				1.7				69% of R			
HF (Cross flow)												
TiO_2/PVP/PVDF/NMP	0.5%	88	78	36	40	Ind. Surf.	COD ~1420 mg/L, pH 6.8, 410 mL/min	8 W UV-A, 36 cm^2	66.7% of R		Under UV-light optimum content of TiO_2 (2 wt%) exhibited desired porosity, hydrophilicity, tensile strength, rejection and long-term stability in salty environment under UV.	[32]
	1%		71		60							
	2%		61		82							
	3%		64		81							
TiO_2/PVP/PVDF/NMP	0.5%			85	85		6.4 mg/L, 250 mL, rate 0.06 m/s (25 g/L NaCl)	UV-A 18 W, 6 h, 36 cm^2			Addition of pore-former PEG, increase the hydrophilicity and and hence improved water permeability and stability of PMs under salty water.	[23]
TiO_2/PVP/PEG/PVDF /NMP	0.5%	86	78	82	83	MB-water			97%	0.012		
						MB-NaCl						
HF (submersed)												
TiO_2/PVDF/DMAc	3%	91	79			NP	100 mg/L, 7 L pH 6.8	UV-A 36 W, 4 h, 248 cm^2 (20 HF)	98% of R		7.5 wt% is the optimum TiO_2 content, and above this value decrease antifouling property, porosity and hence flux performance.	[26]
	7.5%		78						96% of R			
	10.5%		75						91% of R			
	15%		67						96% of R			

TiO_2 nanotube/ PVP/PVDF/NMP	0.1%	76	70		(POME)	TC = 742 mg/L, 15 L. pH 3	UV-A 8W, 4 h, 2.89 m^2	42.3%		The best flux, rejection and anti-fouling property observed for 0.5wt% TiO_2. High initial concentration decreases photoactivity of PMs, and alkaline condition improve flux.	[53]
	0.3%		65					57.1%			
	0.5%		64					67.3%			
	1%		61					50%			

Annex 5 Representative of Some Visible-light sensitive PMs used in different types of PMRs, their Photocatalytic Activity, and Other Performances of Membranes including Operating Conditions

Flat sheet or Hollow fiber membranes in Batch Process

PM type	wt% TiO_2 added	θ (°)		ε (%)		M	C_0 , V_0, pH, υ	I, t, A	D (%) or R (%)	k_{app} (min^{-1})	P (μg/(h ×cm^2))	Observation and other performances	Ref.
		Support	PM	Support	PM								
N-TiO_2/ PEG/PVDF/ DMAc (DLHF)	7.5%		70		35.1	BPA	5 mg/L	30W LED Visible light 6h	81.6%			N-doped TiO_2 DLHF shows the same photoactivity under UV and solar irradiation. 7.5 wt% is the optimum catalyst dose, above this content, properties improve but catalyst agglomerates due to higher surface tension between the solvent of dope solution.	[77]
	3%		82		9.6	RB5	5 mg/L		75% (for 7.5 wt% TiO_2)				[55]
	7.5%		70		35.1								
	10.5%		69		55.1								
Fe-TiO_2/ PEG/PSF/ DMAc & NMP (4:1)	0.05%					BPA	10 mg/L, 100 mL	500 W Xenon lamp, 3 h, 47.78 cm^2	90.8% (for 0.2 wt%)		6.33	Enhanced mechanical property and shows self-cleaning ability under visible-light. Optimum catalyst dose is 0.2 wt%. Higher inclusion of TiO_2 (0.25 wt%) decreases membrane mechanical stability.	[78]
	0.1%												
	0.15%												
	0.2%												
	0.25%												
N–TiO_2/ PMAA-*g*-PVDF/PAN/ DMAc	1%					Bentaz	10 mg/L, 100 mL. pH 7	UV 5063 lux, 3 h, 36 cm^2	42.9% for 3 wt% TiO_2		3.97	3 wt% catalyst dose optimum amount, above this value, roughness of the membrane surface increases because nanoparticles began to form lumps. Under basic conditions, positive charged bentazon adsorb more on PMs surface and enhance photodegradation.	[62]
	3%												
	5%							Sunlight 110000 lux, 3 h, 36 cm^2	99.8% for 3 wt% TiO_2		9.24		
Pd/N-TiO_2/ PSf/NMP	0.5%	79	66			EY	100 mg/L, 100 mL	450W Xenon lamp, 3 h, 9 cm^2	92.7%	0.0098	257.5	Improved hydrophilicity, porosity, visible light absorption and photoactivity but higher TiO_2 content increased membrane roughness due to embedded TiO_2 particle aggregation.	[61]
	1%		72						86.7%	0.0084	240.9		
	2%		73						97%	0.0149	269.4		
	4%		76						96.3%	0.0142	267.5		
	7%		77						97.3%	0.0169	270.3		
Flat sheet (Dead-end)													
Ag-TiO_2/ APTES/PVP /PVDF/DM Ac	0.1%	82	73			MB	3 mg/L, 30 mL. pH 7	Visible light, 1 h	80.3%			Smaller TiO_2 particles caused intracellular damage, and unique antibacterial performance. Meanwhile, Ag has inhibitory effect on the growth of bacteria; Thus these PMs shows excellent antibacterial activity towards E coli. Under visible light, provides a good self-cleaning ability and improved BSA rejection (from 63.43 to 89.80%)	[52]
	0.2%		68						86.7%				
	0.5%		61						90.1%				
Ag-TiO_2/ PVP/PVDF/ DMAc	0.01%	83	78			BSA		450 W Xenon lamp, 9 cm^2	97.21% of rejection, 8h				[59]
	0.03%		74										
	0.06%		57										

RGO-Ag-TiO_2/PEG/GLUT/CA	2.5 mg[†]		66		MB	20 mg/L	500 W Xenon lamp,	99% of rejection for all pollutant conditions			Inclusion of 10 mg of catalyst shows good and stable hydrophilicity and water permeability. Simultaneously degrade dye and separate oil–water emulsions under visible-light irradiation in a short time.	[58]
	5 mg		59		MB-oil							
	10 mg		43		RhB	30 mg/L						
	20 mg		37		RhB-oil							
mpg-C_3N_4/TiO_2/PVP/PSf/NMP	0.2%	71	66		SFMO	10 mg/L, 50ml	300 W Xenon lamp, 30 h, 8.5 cm^2	49%		0.96	Mechanically stable PMs prepared by adding nanoparticles. Increase hydrophilicity of the PMs, enhance water permeability albeit pore size decreased.	[60]
	1%		58					69%		1.35		
Flat sheet (Cross-flow)												
TiO_2/PVDF-TrFE/DMF	8%				Tartz	10 mg/L	Sunlight, 5 h, (38×12) cm^2 υ = 28 mL/s (for all C_0)	77.77	0.30		Increase in initial feed concentration (10-30 mg/L) reduced the photodegradation of tartzarine (78 to 47%). Meanwhile, increasing the feed flow rate (9.78-28 mL/s) enhance photodegradation efficiency (37-77%) due to larger turbulence from the higher flow rate, which promotes external mass transfer.	[33]
						20 mg/L		57.72	0.18			
						30 mg/L,		46.57	0.12			
3D-TiO_2/ZnO/PVDF (ALD)		95	40		MB	3.2 mg/L, 100 mL 300 mL	200 W Xenon lamp, 19.6 cm^2	95% (30 min)	0.11	31.02	Super-hydrophilicity of this visible-light active membrane shows enhanced anti-fouling performance.	[57]
					HA			73% (1 h)		35.75		
L–Histidine/TiO_2/CdS/PVP/PES/DMAc	0.1%	63	51		POME	1 g/L, pH 5.5, 150 L/h	500 W Halogen lamp,	100% (30 min)			Better performance observed after incorporation of 0.5 wt% catalyst, because above this load surface becomes rougher and nanoparticle agglomerates. Increase in initial feed concentration (1-5 g/L) reduced the permeation flux (31.4 to 11 $kg/m^2.h$). Meanwhile, increasing the feed flow rate (50, 150 L/h) also improved rejection efficiency and permeation flux. Due to turbulence as well as bigger Reynolds number from higher flow rate reduce the concentration polarization and membrane fouling.	[79]
	0.5%		47									
	1%		45									

[†] These amounts are deposited onto membrane grafting by PEG and GLUT through vacuum filtration method

[**] These are based on suspensions of TiO_2 on water and then membrane was immersed in this suspension to deposit TiO_2

Annex 6 Recipient to crystallize on-site synthesized TiO_2 nanoparticles on membrane

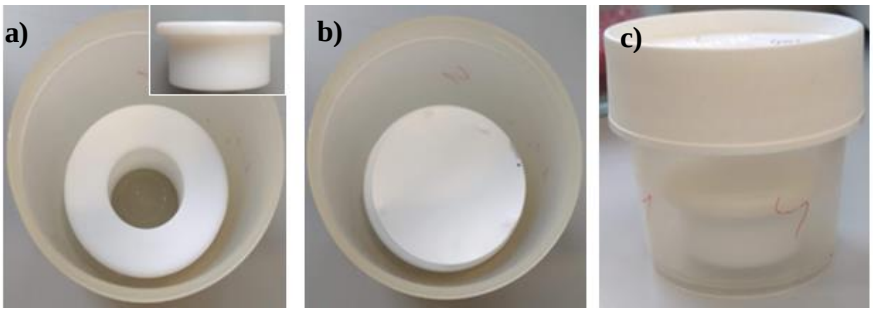

Annex 7 SEM images of the Membranes prepared from lower concentration (2 mM and 4 mM) sol-gel solution; a) Pure PVDF (0mM), b) 2mM, c) 4mM

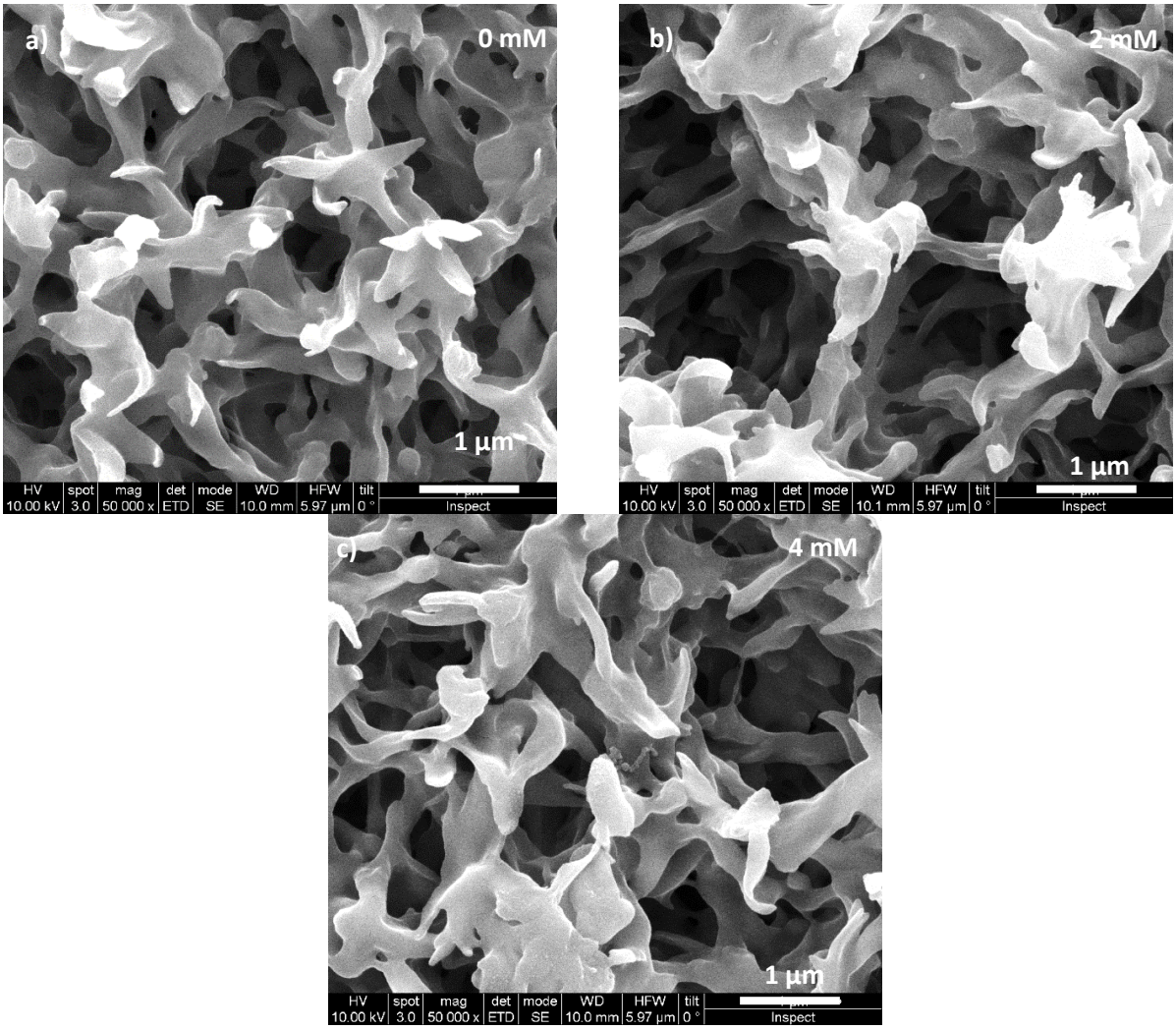

Annex 8 Histogram of the distribution of diameter of nanoparticles deposited on a) 8mM, b) 16mM, and c) 32mM

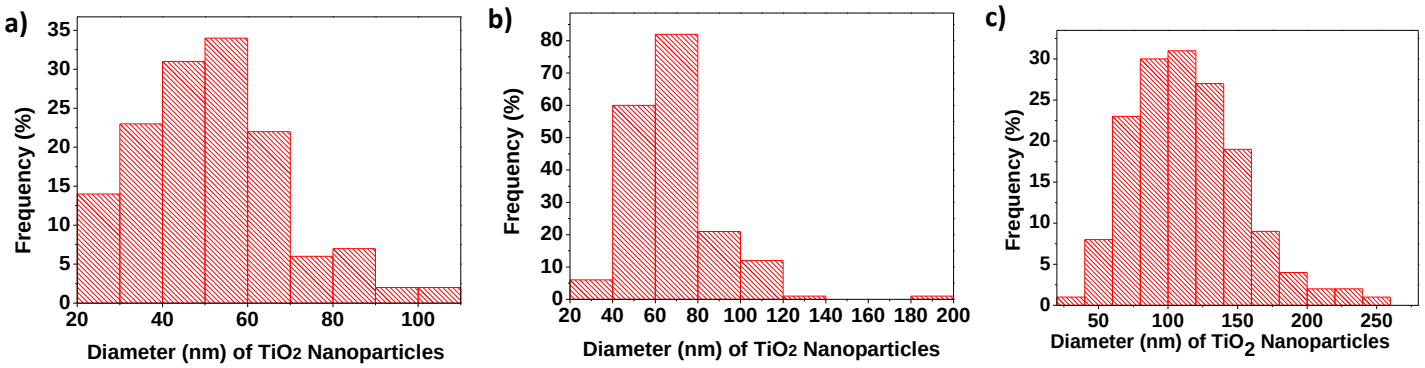

Annex 9 Effect of Mechanical Stirring on MB adsorption onto non-coated pure PVDF membrane a) adsorption at 200 rpm for 3 runs, b) adsorption at 300 rpm for 2 runs, c) adsorption at 400 rpm, and d) comparison of average adsorption rates for all runs.

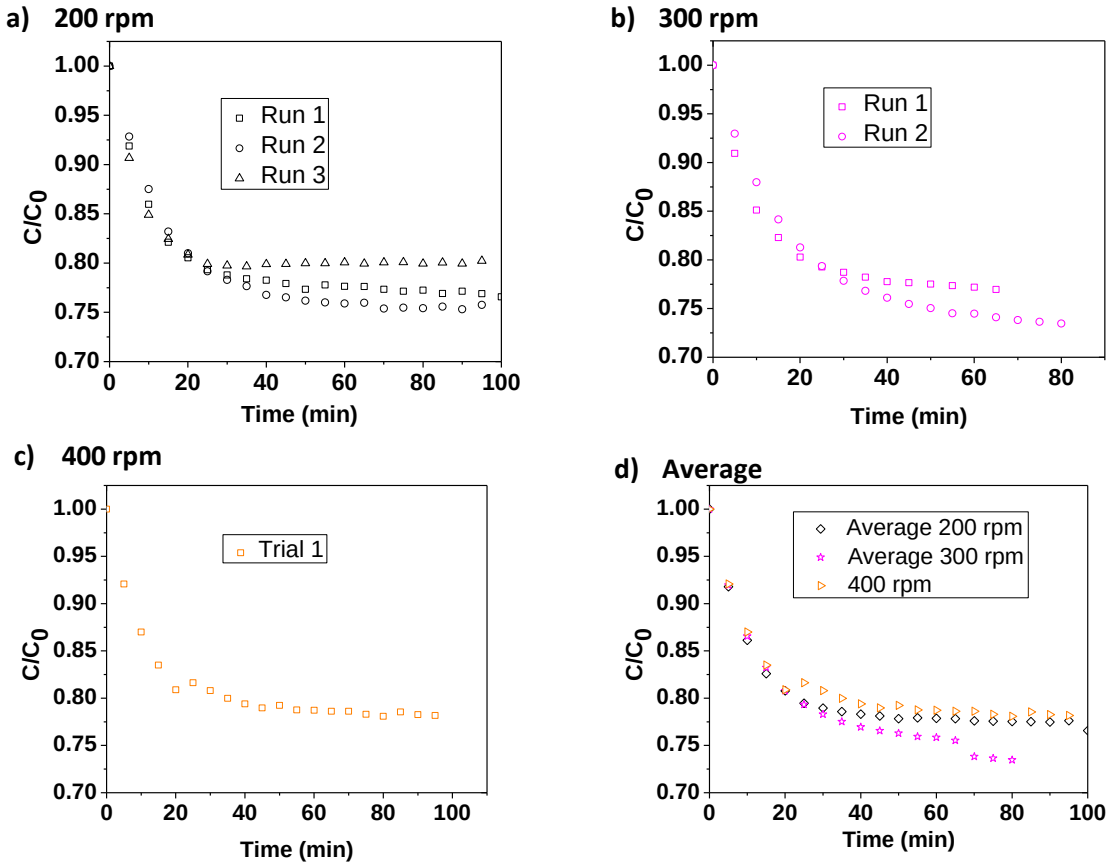

Annex 10 Histogram of the distribution of diameter of nanofibers of a) Electrospun pure PVDF, b) PPTM, and c) PTM